J Geophys (1985) 58:175–182

Journal of Geophysics

Focal parameters of some Friuli earthquakes (1976–1979) using complete theoretical seismograms

M.S. Barbano [1], R. Kind [2], and G. Zonno [3]

[1] Istituto di Scienze della Terra, viale Ungheria 43, 33100 Udine, Italy
[2] Seismologisches Zentralobservatorium, Krankenhausstraße 1, 8520 Erlangen, Federal Republic of Germany
[3] Istituto per la Geofisica della Litosfera Reparto Terremoti – C.N.R., via Bassini 15, 20133 Milano, Italy

Abstract. The relocation of a number of large shocks and the estimation of their fault-plane dip, along with seismotectonic evidence, allow some conclusions about the mechanisms of Friuli (NE Italy) earthquakes. The largest shocks of the 1976 sequence are located in an area with an ESE-WNW trend, extending on both sides of the Tagliamento River. The May earthquakes occurred over the whole area, while the September aftershocks were concentrated in the centre of this area. The 1977–1979 events are spread over a wider zone. These shocks can be ascribed mainly to Dinaric structures. The hypocentre distribution of the largest 1976 events shows that the stress involved deeper crustal sectors in the south of this area (about 8 km) than in the northern part (where it does not exceed 6 km). The motion occurred either in the south along gently dipping planes, which probably correspond to the detachment surface between the post-Hercynian cover and the Paleozoic basement, or in the north along more steeply dipping planes (thrusts) within the Mesozoic cover, along with triggering and rearrangement in the shallower Alpine and/or Dinaric structures.

Kew words: Friuli earthquakes – Fault-plane determination – Theoretical seismograms

Introduction

The main aim of this paper is to redetermine the hypocentral distribution and to summarize some aspects of focal mechanisms of the largest Friuli shocks in the years 1976–1979. The correct determination of the rupture zone and of the focal mechanisms is fundamental to the understanding of the relationship between seismicity and tectonics.

The data for this work came mainly from the digitally recording broadband Gräfenberg (GRF) array, described by Harjes and Seidl (1978). This array is located at a distance of about 450 km from the epicentral area of the events considered. At this distance it is usually difficult to identify later phases at single narrow-band stations. Correlation over an array and the possibility of applying different filters to broadband data allow later phases to be identified at regional distances and interpreted using complete theoretical seismograms.

Zonno and Kind (1984) determined the relative source depth of these earthquakes using P_n and sP_n phases. The amplitude ratio of these two phases strongly depends on source orientation.

In order to estimate the most probable source orientation for the Friuli earthquakes, we attempt to model the P_n and sP_n phases with theoretical seismograms. Fault-plane solutions have already been estimated for these earthquakes. However, whereas the solutions for the larger events are reliable, some ambiguities exist for the smaller events. It is therefore difficult to correlate their source orientation with tectonic structures.

It is not possible to resolve fault-plane solutions with one station; but we can estimate, as we will see, the fault-plane dip.

Epicentral distribution

First, the available information on epicentral location was analysed. In fact there is some doubt concerning the location of the 1976 main shock. The shocks were relocated in this study using the Hypo71 program (Lee and Lahr, 1975). The computation has been performed using the Angenheister et al. (1972) crustal model and stations within a range of 500 km from the epicentral area. The focal depths were fixed on the basis of the results of Zonno and Kind (1984).

The events (Table 1) are located in an area with ESE-WNW trend (Fig. 1), extending on both sides of the Tagliamento River. The main shock (6 May 1976, hr:20.00) and its foreshock hr:19.59) are located on the eastern edge of the aftershock distribution near the Cagnetti and Console (1977) and CSEM location and not in the centre (Istituto Nationale di Geofisica, Roma).

The May events are distributed over the whole region, while the September aftershocks occurred in the middle of this area. The 1977–1979 earthquakes are spread over a wider zone (Slejko and Renner, 1984).

Moreover, it seems that there is no correlation between depth and areal distribution of the epicentres. The epicentral distribution obtained agrees with recent redeterminations performed using other methods (Cipar, 1980; Lyon-Caen, 1980; Slejko and Renner, 1984).

Offprint requests to: G. Zonno

Table 1. Earthquake parameters

No.	Date	hr min	Lat. N	Lon. E	*M* S-R	Depth	(km) GRF
1[a]	27.03.28	08.32	46 26	13 03	5.5	4	
2[a]	08.06.34	03.18	46 18	12 28	3.8	6	
3[a]	18.10.36	03.10	46 06	12 26	5.3	7	
4[a]	05.11.56	19.45	46 33	12 57	3.7	7	
5[a]	26.04.59	14.45	46 28	13 00	4.5	5	
6[c]	24.03.75	02.33	46 17	13 08	4.1		
150	06.05.76	19.59	46 17.04	13 20.86	4.5	10[b]	8
15	06.05.76	20.00	46 16.51	13 14.80	6.4	7[b]	6.5
16	07.05.76	00.23	46 15.23	13 20.53	4.5	9[b]	8.5
160	09.05.76	00.53	46 12.89	13 19.60	5.3	6[b]	8.5
17	11.05.76	22.44	46 15.62	13 02.46	4.8	9[b]	6
18	11..09.76	16.31	46 16.50	13 13.47	5.1	6[b]	6.5
20	15.09.76	03.15	46 17.05	13 10.43	5.8	6[b]	5
21	15.09.76	04.38	46 18.61	13 10.13	4.7		8
22	15.09.76	09.21	46 18.02	13 08.74	6.1	11[b]	7
14	16.09.77	23.48	46 16.10	13 00.98	5.2		8
26[a]	12.12.78	15.14	46 19	12 42	4.4		
11	18.04.79	15.19	46 21.27	13 17.77	4.8		5

[a] Kunze (1982); S-R: Slejko and Renner (1984)
[b] EMSC
[c] Mayer-Rosa et al. (1976)
GRF = Zonno and Kind (1984)

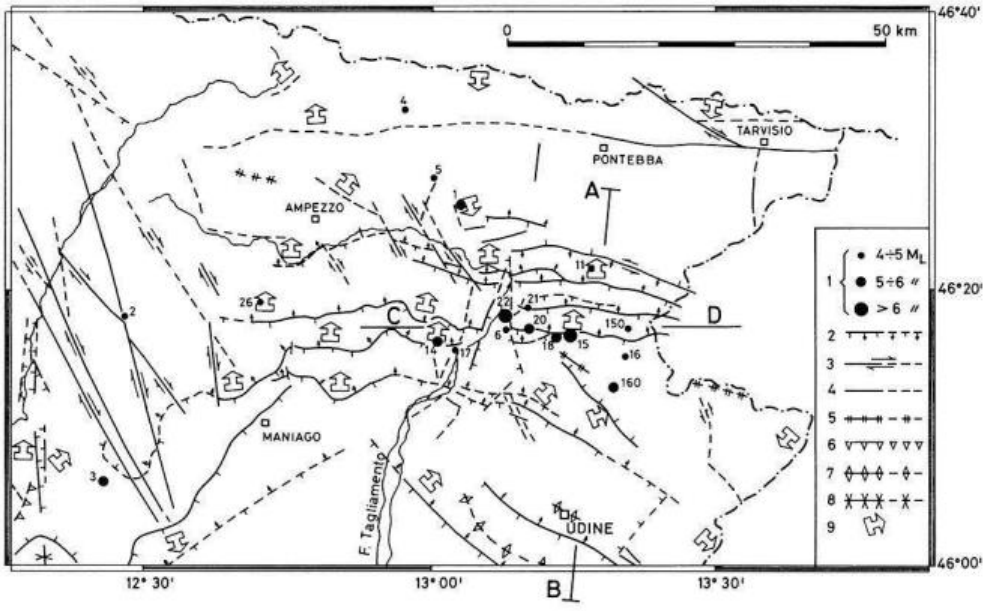

Fig. 1. Main neotectonic structural features, upper Pleistocene-Holocene (after Zanferrari et al., 1982; modified), and epicentral distribution. *AB* and *CD* cross-sections of Figs. 10 and 12. 1: epicentres; 2: dip-slip fault (*dashes* towards lowered area, *arrows* according to the dip direction); 3: strike-slip fault; 4: fault with undetermined character; 5: uplifting axis; 6: flexure; 7: anticline axis; 8: syncline axis; 9: asymmetrical uplift (*arrow* towards less uplifted area)

Tectonic setting and fault-plane solution (FPS)

The shocks we are dealing with are located in Friuli, in the eastern part of the Southern Alps, where the overlap with Dinaric structures takes place.

The Southern Alps are interpreted, in global tectonics, as the result of the continuation of relative motion between the European plate and the Adriatic microplate, and the Alps originate from their collision in the late Cretaceous-Tertiary.

These movements, as demonstrated by neotectonic structures and by seismic activity, are still active. But, the subduction process must already be completed and the suture between the European continent and the Adriatic plate has already occurred, as shown by deep crustal seismic sounding profiles (Italian Explosion Seismology Group and Institute of Geophysics, ETH Zürich, 1981) and by the hypocentre distribution of earthquakes which occur only in the upper 15 km of depth (Siro and Slejko, 1982).

The northward movement of the Adriatic plate in the Neogene and Quaternary involved increasing areas of the Southern Alps. This should have caused intense shortening, mainly in post-Hercynian cover, with a build-up of overthrusts verging towards the south and its probable detachment from the Paleozoic basement in the more southern sector. In the pre-alpine area especially, the Dinaric overthrusts have been partly split up and incorporated in the south-Alpine overthrusts and partly re-utilized in the south-Alpine tectogenesis, causing very complicated structural relationships (Zanferrari, personal communication).

Table 2. Fault-plane solutions

No.	Date	hr min	Plane A		Plane B		Ref.
			Dip	Strike	Dip	Strike	
1	27.03.28	08.32	90	112	90	202	K
2	08.06.34	03.18	82NNE	295	70WNW	203	K
3	18.10.36	03.10	88NNE	293	60WNW	200	K
4	05.11.56	19.45	90	94	90	184	K
5	26.04.59	14.45	76NNE	305	70WNW	210	K
6	24.03.75	02.33	60NE	316	69WNW	212	M-R
60	24.03.75	02.33	54SSE	81	36NNW	261	M-R
150	06.05.76	19.59	72S	86	22NW	230	S-R
			19E	353	84NNW	244	CON
15	06.05.76	20.00	70SSE	78	22NW	230	S-R
			75SSE	76	15N	266	C
			78S	80	16NW	222	L-C
16	07.05.76	00.23	70S	86	34NW	208	S-R
			15ESE	22	78NW	237	CON
	08.05.76	03.10	60SSE	82	30NNW	256	S-R
160	09.05.76	00.53	56SSW	100	34N	266	S-R
			28E	15	64NW	221	CON
	10.05.76	04.35	64SSE	72	26NNW	244	S-R
17	11.05.76	22.44	62SSE	96	30NNW	252	S-R
			88S	94	4WNW	198	DCP
	08.06.76	12.14	62SSW	104	44NW	226	S-R
	26.06.76	11.13	70S	90	34WNW	212	S-R
	14.07.76	05.39	62SSW	102	44NW	224	S-R
18	11.09.76	16.31	62SSE	82	36NW	220	S-R
			33S	89	62NW	233	CON
	11.09.76	16.35	76SSE	76	14NW	234	S-R
	12.09.76	19.53	66S	90	24NNW	254	S-R
	13.09.76	18.54	64SSW	96	42NW	218	S-R
20	15.09.76	03.15	46SE	30	46NW	232	S-R
			58ENE	350	56NW	235	L-C
			50ENE	349	60NW	230	C
21	15.09.76	04.38	80SE	52	14W	186	S-R
22	15.09.76	09.21	50S	84	40N	264	S-R
			68SE	56	30NNE	278	C
			68SE	56	24NNW	260	L-C
	15.09.76	09.45	66SSW	100	50NW	212	S-R
	15.09.76	19.31	62SSW	98	36NW	234	S-R
	03.04.77	03.18	60SW	140	31NE	302	S-R
14	16.09.77	23.48	72S	92	22NW	234	S-R
			68ENE	349	68NNW	249	K
	20.02.78	12.13	90	276	14E	6	S-R
	03.04.78	10.49	57SW	144	42NNE	280	S-R
26	12.12.78	15.14	64SSE	82	26NNW	252	S-R
			74SSE	82	40WNW	192	K
	06.03.79	13.46	40SW	136	52NE	292	S-R
11	18.04.79	15.19	58SE	68	62NE	316	S-R
			90	171	90	261	K
	19.06.79	10.03	70S	82	40WNW	196	S-R
	14.08.79	18.58	48N	268	80E	6	S-R

K: Kunze (1982); M-R: Mayer-Rosa et al. (1976); S-R: Slejko and Renner (1984); C: Cipar (1980); L-C: Lyon-Caen (1980); DCP: D'Ingeo et al. (1980); CON: Console (1976).
The dip is the angle which the fault plane forms with the horizontal. The strike is the azimuth, north through east, of the fault plane

The most important regional structural features are (Fig. 1): the E-W-striking south-Alpine overthrusts (mainly in the northwest) and the SE-NW-striking Dinaric overthrusts (mainly in the southeast and buried in the Friuli plane). These structures are intersected by subvertical faults, striking about N-S and often showing strike-slip motion. Both structures (overthrusts and strike-slip faults) are compatible with the actual stress field, with NNW-SSE maximum compressive stress (Zanferrari et al., 1982). The earthquakes before the 1976 events have FPS showing mainly strike-slip motion (8 June 1934, 18 October 1936 Cansiglio; 27 March 1928, 5 November 1956, 26 April 1959 Tolmezzo), on planes with prevailing directions between E-W and WNW-ESE or between N-S and NNE-SSW (Table 2).

The FPS of the 24 March 1975 earthquake is ambiguous, because of its small magnitude; it may be either a strike-slip mechanism, with a NNE-SSW- or NNW-SSE-striking plane, or a thrust mechanism, with nearly E-W-striking plane (Mayer-Rosa et al., 1976).

For the 6 May 1976 (hr:19.59) foreshock and the 16 September 1977 event, several solutions exist (Table 2). Some authors give a strike-slip mechanism, others a thrust mechanism.

The main shock (6 May 1976, hr:20.00) and the 15 September 1976 (hr:09.21) aftershock have a similar mechanism of thrust type; the gently northward-dipping nodal plane, striking nearly E-W, is chosen as the fault plane (Müller, 1977a; Cipar, 1980; Slejko and Renner, 1984).

The mechanism of the 15 September 1976 (hr:03.15) aftershock again shows dip-slip motion but with a considerable strike-slip component. The nodal planes strike NE-SW and N-S, in contrast to the other mechanisms in which the nodal planes strike nearly E-W (Cipar, 1980; Lyon-Caen, 1980). Furthermore, this aftershock is located at a shallower depth than the previous events (Lyon-Caen, 1980; Zonno and Kind, 1984).

Most of the May-September 1976 aftershocks have FPS of thrust type with nodal planes striking E-W, whereas the following events show different mechanisms. There are either transcurrent or thrust mechanisms as well as normal mechanisms (Slejko and Renner, 1984). For the thrust earthquakes, the available data define the steeply dipping nodal plane quite well, while the other plane is almost completely unconstrained.

For most earthquakes, either with thrust or strike-slip mechanism, the maximum compressive stress is oriented between NW-SE and N-S, in agreement with the regional neotectonic stress field (Zanferrari et al., 1982).

Three zones with different types of mechanism can be distinguished:

1) to the north of the Periadriatic overthrust and to the west of the Tagliamento River, the earthquakes show mainly transcurrent motion. The maximum compressive stress axis, P, is oriented NNW-SSE- These mechanisms are related mostly to events before and after the 1976 sequence (Fig. 2a and d).

2) In the contact zone between Julian and Carnic pre-Alps (Gemona, Buia, Osoppo area), the mechanisms are of thrust type but with a strike-slip component. The P trend is NW-SE (Fig. 2c) and the nodal planes strike nearly N-S.

3) To the south of the Periadriatic overthrust and to the east of the Tagliamento River, the FPS are of thrust type with a gently dipping nodal plane striking nearly E-W. P is oriented nearly N-S (Fig. 2b and c). These earthquakes seem to be located at a deeper seismic level (7–10 km) than the transcurrent ones (4–6 km), located in the first zone.

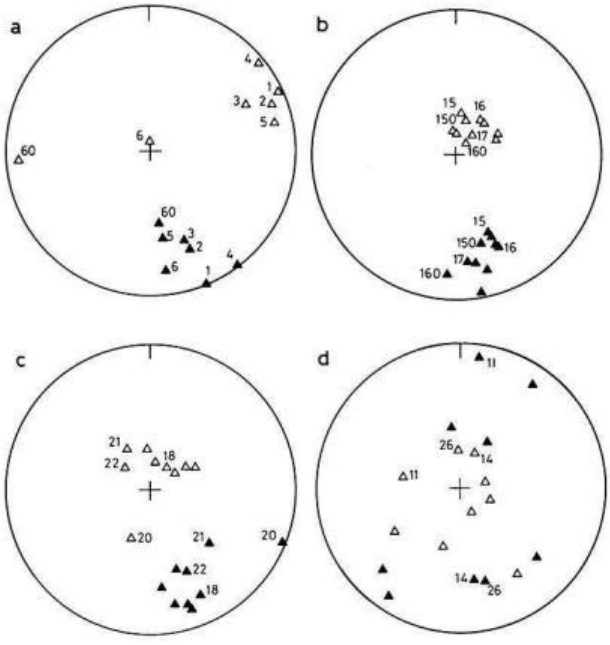

Fig. 2a–d. Composite plot of principal stress axes P (▲) and T (△) for the available fault-plane solutions: **a** events before 1976; **b** May-August 1976 events; **c** September-October 1976 events; **d** events after 1976

Analysis and results

The theoretical seismograms have been computed using a modification by Kind (1978, 1979) of the original reflectivity method of Fuchs (1968). The method allows computation of complete theoretical seismograms for a point source buried in a horizontally layered medium.

The source is a dislocation point source, whose orientation is defined by three angles: the strike θ, the dip δ, and the slip λ, according to the FPS. Φ is the azimuth between the strike of the fault and the station. The moment function used was taken from Brüstle and Müller (1983). The spherically layered earth is mapped into a plane-layered medium using an earth-flattening approximation (Müller, 1977b), although this effect is small for the distances considered.

To fit the data, a modification of the Angenheister et al. (1972) crustal model has been used (Fig. 3). A linear velocity variation between 7 and 7.8 km/s is considered from 42 to 50 km. Q values of 1,000 for P waves and 300 for S waves were assumed for the whole model. The shear velocities are obtained by dividing the P velocities by the square root of 3.

The P_n and sP_n phases are not very dependent on the model assumed. These phases travel at the Moho and are not influenced much by the complex structure of the Alpine crust. The path at the Moho is the same for P_n and sP_n. Both phases are therefore influenced by a complex Moho in the same way. The two phases have different paths only in a relatively small region near the source (Zonno and Kind, 1984). The crustal model of Angenheister et al. (1972) has been selected because it acceptably reproduces the

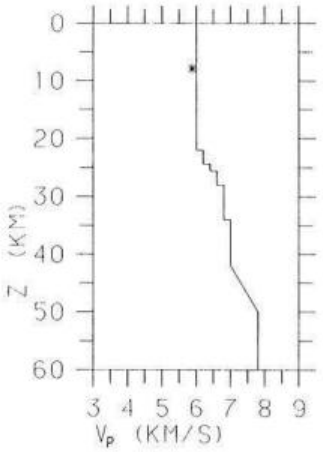

Fig. 3. Crustal model used (after Angenheister et al. 1972, modified). The source depth used for the test computations is indicated by the *asterisk*

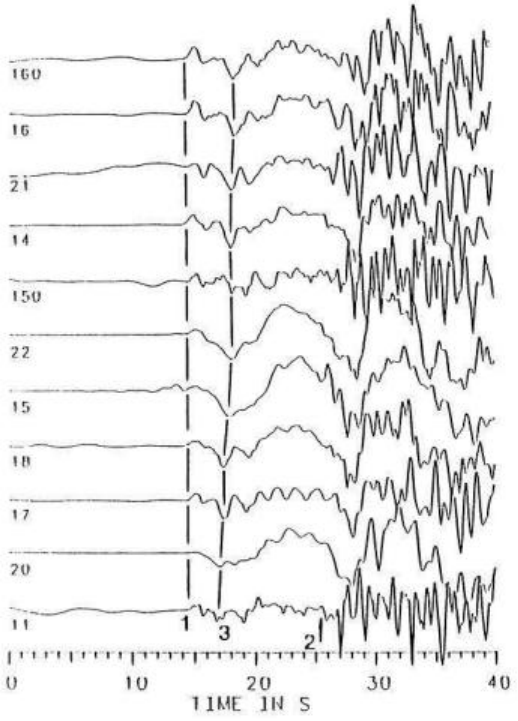

Fig. 4. Displacement-proportional records of GRF array station A1, vertical component. The parameters of the events are given in Table 1. P_n and P_g are marked 1 and 2, respectively. 3 is the depth phase sP_n. The records are sorted so that the time differences sP_n-P_n increase from the bottom to the top of the figure. These differences depend on the source depth (after Zonno and Kind, 1984)

phases considered. The displacement-proportional Kirnos filter has been used to compute theoretical seismograms.

Figure 4 shows displacement-proportional records of the GRF station A1 of the largest Friuli events (Table 1). Phases marked 1 and 2 are P_n and P_g, respectively. According to earlier work by Zonno and Kind (1984), the phase marked 3 is the depth phase sP_n. The records are sorted so that the time differences between sP_n and P_n increase from the bottom to the top of the figure. These differences

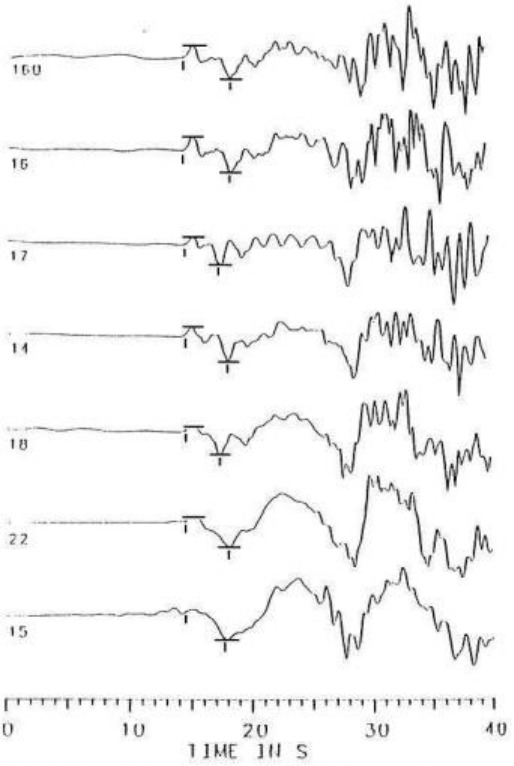

Fig. 5. Events from Fig. 4 with similar waveforms and source orientation (see Table 2). The records are sorted so that the amplitude ratio of P_n/sP_n increases from the bottom to the top of the figure. This variation depends on the source orientation

depend on the source depth. Some of these earthquakes have similar signal form and frequency. The events 160, 16, 17, 14, 18, 22 and 15 have similar FPS of thrust type with a steeply dipping E-W plane and a nearly horizontal plane not always well constrained. These records are sorted in Fig. 5 so that the amplitude ratio P_n/sP_n increases from the bottom to the top. The amplitudes of P_n and sP_n are measured from the zero line to the maximum. The amplitude ratio of these two phases depends on the source orientation.

Several tests have been performed to investigate the influence of the source orientation on the signal form, starting from an average source orientation, $\theta = 96°$, $\delta = 16°$ N ($\delta = -16°$) and $\lambda = 80°$, assumung a rise time of 1.2 s and a source depth of 8 km. This average source orientation is similar to Cipar's (1980) orientation ($\theta = 86°$, $\delta = 15°$ N, $\lambda = 80°$). The strike of our average orientation corresponds to an azimuth (Φ) of $-116°$ to Gräfenberg. The amplitudes are normalized. No moment determination was attempted. Using only single-station data, it is difficult to estimate the seismic moment and energy of an earthquake because of the corrections necessary for source mechanism and propagation path. In particular the effects of pP and sP interference and the effects of the structures at the source and receiver sites are very critical points (Seidl and Berckhemer, 1982).

The fit between observed and computed seismograms is good during the first 10 s. This can be seen in Fig. 6, where the theoretical seismogram at about 412 km and the record of earthquake 14 are compared. We have varied

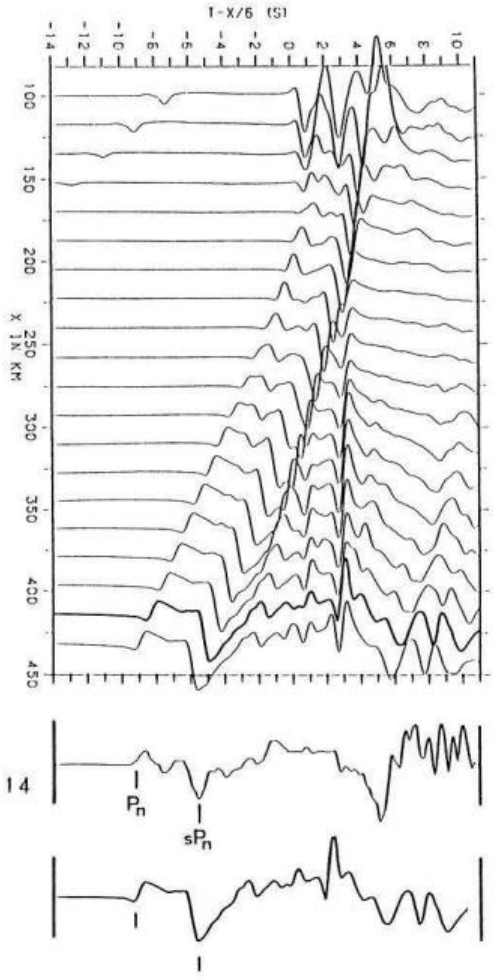

Fig. 6. *Top:* Theoretical seismograms, computed according to an average source orientation, as a function of epicentral distance; $\lambda = 80°$, $\delta = 16°$ N, $\theta = 96°$ (the angle Φ between the strike and GRF is $-116°$), depth 8 km. *Bottom:* Comparison between the theoretical seismogram at about 412 km distance (*heavy line*) and the observed seismogram of earthquake 14

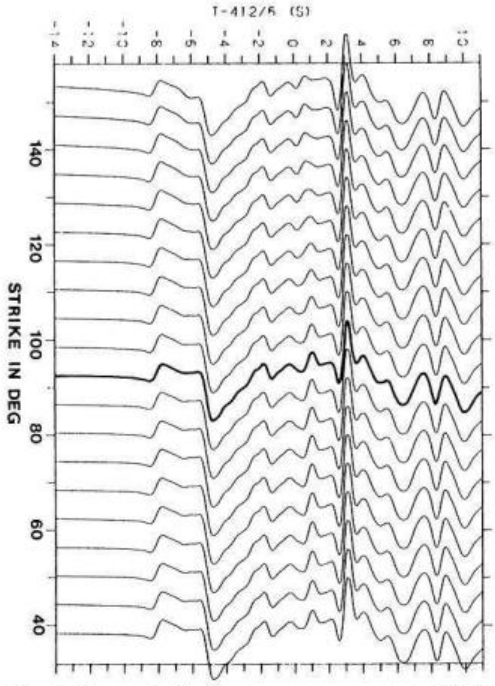

Fig. 7. Theoretical seismograms computed with fixed slip ($\lambda = 80°$), dip ($\delta = 16°$ N) and varying strike $152° > \theta > 40°$ of the fault. The seismogramm drawn with a *heavy line* in Figs. 7, 8 and 9 corresponds to our average source orientation

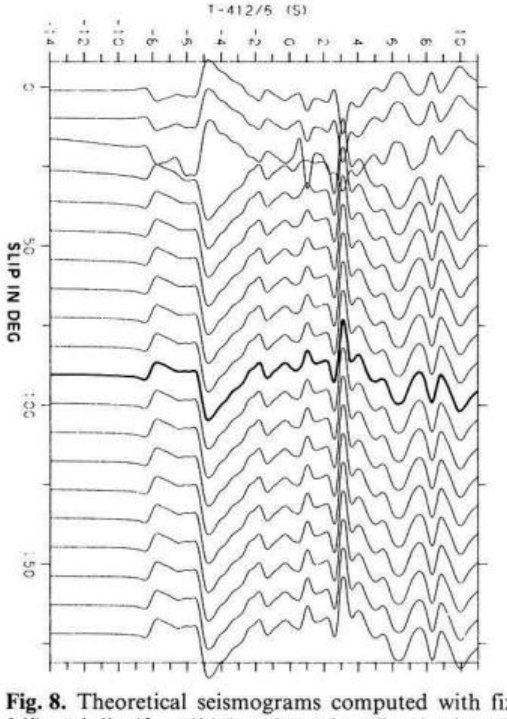

Fig. 8. Theoretical seismograms computed with fixed strike ($\theta = 96°$) and dip ($\delta = 16°$ N) and varying slip $0° < \lambda < 180°$

the source orientation in order to estimate how much this influences the signal forms. Two angles were kept fixed in each experiment and the third was varied. This procedure does not cover the complete space of the three angles, but it seems to be sufficient for an estimate. The variation of strike, $40° < \theta < 152°$ ($\lambda = 80°$, $\delta = -16°$) has little influence on the computer theoretical signal forms (Fig. 7). The variation of the slip vector in Fig. 8, $0° < \lambda < 180°$ ($\delta = -16°$, $\theta = 96°$), shows an inversion point at 20°, otherwise the waveform is quite similar.

A more meaningful result is derived from the dip variations. Figure 9 shows that the P_n phase disappears when the dip varies from $0° < \delta < 45°$ N ($\lambda = 80°$, $\theta = 96°$). So the slightly varying P_n/sP_n amplitude ratio is interpreted as a slightly varying dip of the fault plane.

A good fault-plane dip estimation for the earthquakes of Fig. 5 can be obtained by comparing the P_n/sP_n ratio between observed and computed seismograms. The earthquakes 160, 16, 17, 14 have a fault plane with a smaller dip (between 3° N and 11° N) than the earthquakes 15, 18 and 22, whose dip is between 15° N and 25° N. Furthermore, the shocks 160, 16, 14 are located at greater depth (at about 8 km) than the shocks 15, 17, 18 and 22 (at about 6 km), see Fig. 10. The two shocks 11 and 150 contain higher frequencies than the rest of the events in Fig. 4. The two FPS for shock 11 are similar (Table 2); the mechanism is strike-slip. In contrast, several solutions exist for foreshock 150. It is possible that the higher frequencies of these

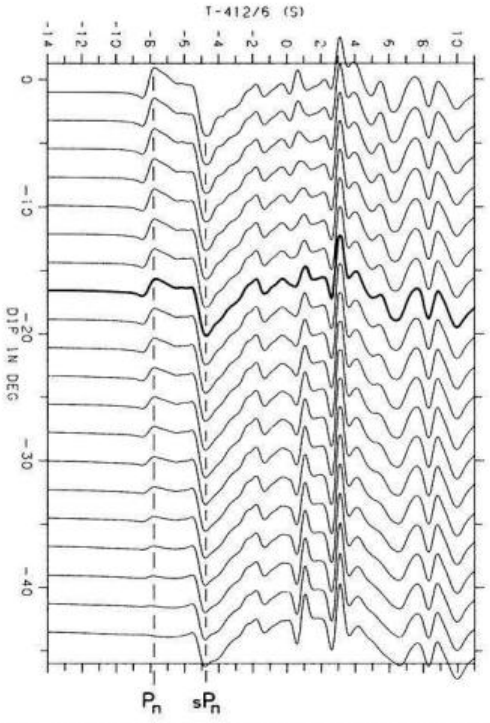

Fig. 9. Theoretical seismograms computet with fixed slip ($\lambda = 80°$) and strike ($\theta = 96°$) and varying dip $0° > \delta > -45°$

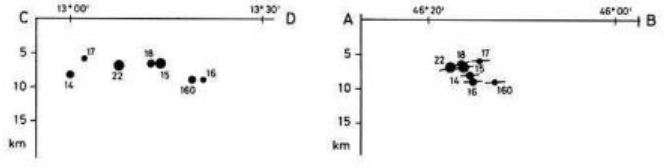

Fig. 10. *Left:* E-W cross-section with hypocentre distribution. *Right:* N-S cross-section with hypocentre distribution and fault-plane dip (see Fig. 1)

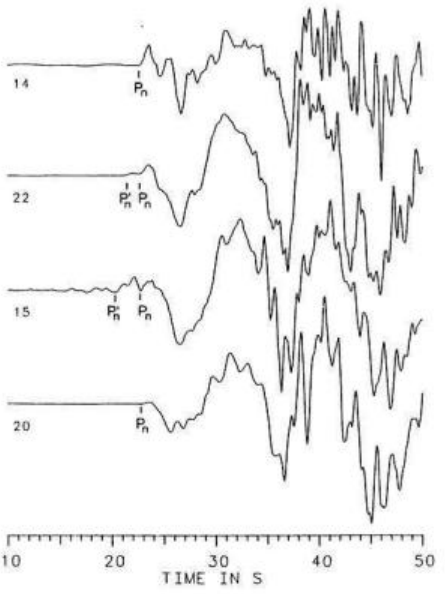

Fig. 11. Representation of P_n onsets for single events (14 and 20) and multiple events (15 and 22)

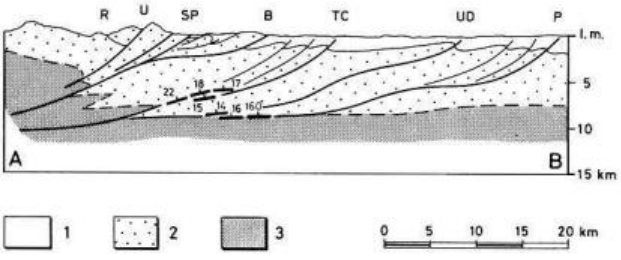

Fig. 12. Attempt at seismotectonic interpretation for the central Friuli region, with the estimated fault-plane dip of the Fig. 5 events. 1: Quaternary and Cenozoic; 2: Mesozoic and Paleozoic with Alpine orogenesis; 3: Paleozoic with Hercynian and Alpine orogenesis and metamorphic basement. R: Resia overthrust; U: Uccea overthrust; SP: Periadriatic overthrust; B: Bernardia overthrust; TC: Tricesimo-Cividale overthrust; UD: Udine-Buttrio overthrust; P: Palmanova overthrust

two shocks are due to different rupture processes and to their smaller magnitudes.

Our theoretical seismograms are computed using a single point source. This is a good approximation since most of the earthquakes of Fig. 4 seem to be single-shock events. The phases P_n and sP_n are easy to identify. Single and multiple events are shown in Fig. 11. For the earthquakes 15 and 22 two P_n onsets can be related to multiple events (see also Cipar, 1981). Cipar also models event 20 as a multiple event although, as he says, the long-period P waves are obscured in many cases by the coda of earlier teleseisms. From GRF data, there is no evidence that earthquake 20 is a multiple event.

Discussion and conclusions

The method used in this work to determine the source orientation does not allow an unambiguous determination of fault-plane solutions because of the influence of other parameters, such as the complicated earth model or the use of a single station. Furthermore, there is evidence for a multiple-event nature for some Friuli earthquakes. Nevertheless, P_n and sP_n modelling for a single station at a regional distance from the epicentre can be a reliable method for the estimation of the fault-plane dip even for small events.

The results obtained are useful for seismotectonic considerations. On the basis of the dip values derived in this study, depth and epicentral distributions and on the basis of the geometry of the faults outcropping in the area, we can suppose that:

The large shocks of May-September 1976 sequence are mainly related to Dinaric structures involved in the south-Alpine shortening (Tricesimo-Cividale, Udine-Buttrio, Palmanova overthrusts), and the stress mainly in the south involved a deeper crustal sector (about 8 km) relative to the more northern part where it appears not to exceed 6 km. The motion occurred either in the south along gently dipping planes, which probably correspond to the detachment surface between the post-Hercynian cover and the Paleozoic basement, or in the north along steeper dipping planes (thrusts) within the Mesozoic cover.

These movements give rise to subsequent triggering and rearrangement in the shallower Alpine and/or Dinaric

structures, along with scattered earthquakes over a wider area.

The cross-section in Fig. 12 shows an attempt at a seismotectonic interpretation for the central Friuli region.

All the earthquakes known in the area have depths of less than 15 km. Therefore, the movements occur only in the upper crust, involving at most the upper part of the crystalline basement beneath the Paleozoic with Hercynian and/or Alpine tectogenesis.

In the Friuli region, the main shocks are often followed several months later by strong aftershocks. The anomalous decay of the aftershocks sequence seems to be a regional seismic peculiarity and is probably due to the alternate movements between Dinaric and Alpine structures, in response to the acting stress. Several examples are reported in the chronicles: the earthquakes which hit Idria and Cividale on March 26, 1511, and struck Cividale again in the same year on August 8; the Tolmezzo earthquake of 1788 followed by another earthquake in 1789 at Tramonti and again at Tolmezzo in 1790 (Carulli et al., 1982); and lastly the better known 1976 sequence.

Acknowledgements. The authors are indebted to D. Slejko for data from Italian and foreign stations. They wish to thank A. Zanferrari for discussions and comments on geological features.

This research was supported by the Italian National Research Council (in the frame of the G.N.D.T., U.O. 1.4.; this paper is contribution number 4) and by the German Research Association (DFG).

References

Angenheister, G., Bögel, H., Gebrande, H., Giese, C., Schmidt-Thome, P., Zeil, W.: Recent investigations of surficial and deeper crustal structures of the Eastern and Southern Alps. Geol. Rundschau. **61**, 349–395, 1972

Brüstle, W., Müller, G.: Moment and duration of shallow earthquakes from Love-wave modelling for regional distances. Phys. Earth Planet. Inter. **32**, 312–324, 1983

Cagnetti, V., Console, R.: Space-time distribution of the Friuli (1976) earthquakes. Ann. Geofis. **30**, 107–184, 1977

Carobene, L., Carulli, G.B., Vaia, F.: Foglio 25 Udine. In: Carta tettonica delle Alpi meridionali (alla scala 1:200,000), A. Castellarin: pp 39–45. CNR, P.F. Geodinamica, Publ. 441, Bologna: Tecnoprint 1981

Carulli, G.B., Giorgetti, F., Nicolich, R., Slejko, D.: Friuli zona sismica: sintesi di dati sismologici strutturali e geofisici. In: Guida alla geologia del Sudalpino centro orientale. Guide geol. reg. S.G.I. A. Castellarin and G.B. Vai: pp 361–370. Bologna 1982

Cipar, J.: Teleseismic observations of the 1976 Friuli, Italy earthquake sequence. Bull. Seismol. Soc. Am. **70**, 4, 963–983, 1980

Cipar, J.: Broadband time domain modeling of earthquakes from Friuli, Italy. Bull. Seismol. Soc. Am. **71**, 1215–1232, 1981

Console, R.: Focal mechanisms of some Friuli earthquakes, 1976. Boll. Geof. Teor. Appl. **19**, 72, 549–558, 1976

D'Ingeo, G., Calcagnile, G., Panza, G.F.: On the fault plane solutions in the Central-Eastern Mediterranean region. Boll. Geof. Teor. Appl. **22**, 85, 13–22, 1980

Fuchs, K.: The reflection of spherical waves from transition zones with arbitrary depth-dependent elastic moduli and density. J. Phys. Earth. **16** (special issue), 27–41, 1968

Harjes, H.P., Seidl, D.: Digital recording and analysis of broadband seismic data at the Graefenberg (GRF) Array. J. Geophys. **44**, 603–612, 1978

Italian Explosion Seismology Group and Institute of Geophysics, ETH Zürich: Crust and upper mantle structures in the Southern Alps from deep seismic sounding profiles (1977, 1978) and surface wave dispersion analysis. Boll. Geof. Teor. Appl. **23**, 92, 297–330, 1981

Kind, R.: The reflectivity method for a buried source. J. Geophys. **44**, 603–612, 1978

Kind, R.: Extensions of the reflectivity method. J. Geophys. **45**, 373–380, 1979

Kunze, T.: Seismotektonische Bewegungen im Alpenbereich. Dissertation. Institut für Geophysik der Universität Stuttgart, 1982

Lee, W.H.K., Lahr, J.C.: Hypo 71 (revised): a computer program for determining hypocenter, magnitude and first motion pattern of local earthquakes. U.S. Geological Survey open file report, 75–311, Menlo Park, 1975

Lyon-Caen, H.: Séisme du Frioul (1976): Modèles de source à l'aide de sismogrammes synthétiques d'ondes de volume. Thèse Diplome de docteur de 3ème cycle. Université Paris VII, 1980

Mayer-Rosa, D., Pavoni, N., Graf, R.: Aftershock-statistics and fault-plane solutions on Friuli earthquakes 1975 and 1976. Boll. Geof. Teor. Appl. **19**, 72, 827–834, 1976

Müller, G.: Fault-plane solution of the earthquake in northern Italy, 6 May 1976, and implications for the tectonics of the eastern Alps. J. Geophys. **42**, 343–349, 1977a

Müller, G.: Earth-flattening approximation for body waves from geometric ray theory-Improvements, corrections and range of applicability. J. Geophys. **42**, 429–436, 1977b

Seidl, D., Berckhemer, H.: Determination of source moment and radiated seismic energy from broadband recodings. Phys. Earth Planet. Inter. **30**, 209–213, 1982

Siro, L., Slejko, D.: Space-time evolution of the 1977–1980 seismicity in the Friuli area and its seismotectonic implications. Boll. Geof. Teor. Appl. **24**, 93, 67–77, 1982

Slejko, D., Renner, G.: La sequenza sismica iniziata con il terremoto del 6 maggio 1976 in Friuli. Convegno: Finalita' ed esperienze delle rete sismometrica del Friuli-Venezia Giulia. Regione autonoma Friuli-Venezia Giulia, Trieste, pp 75–91, 1984

Zanferrari, A., Bollettinari, G., Carobene, L., Carton, A., Carulli, G.B., Castaldini, D., Cavallin, A., Panizza, M., Pellegrini, G.B., Pianetti, F., Sauro, U.: Evoluzione neotettonica dell'Italia nord-orientale. Mem. Soc. Geol. **35**, 355–376, Padova 1982

Zonno, G., Kind, R.: Depth determination of North Italian earthquakes using Graefenberg data. Bull. Seismol. Soc. Am. **74**, 1645–1660, 1984

Received March 19, 1985; revised version June 3, 1985
Accepted June 27, 1985